EFFECTS OF NOCTURNAL VENTILATION AND RADIANT COOLING/ HEATING FLOORS ON INDOOR AIR TEMPERATURES IN AN OFFICE BUILDING IN HOT ARID REGION

G. Alvarez[1], M.J. Jiménez[2], M.R. Heras[2], M.A. Chagolla[3], J. Arce[2]& J.P. Xamán[2]

[1]ME Department, Centro Nacional de Investigación y Desarrollo Tecnológico-TMN-SEP. Morelos. México. Email: gaby@cenidet.edu.mx.
[2] Energy Efficiency in Buildings Unit. Centro de Investigaciones Energéticas, Medioambientales y Tecnológicas. Spain. Email: mjose.jimenez@psa.es
[3]Instituto Tecnológico de Zacatepec-TNM-SEP. Morelos, Mexico.

Abstract

The effects of nocturnal ventilation and radiant cooling/heating floors on indoor air temperatures in an office building in hot arid region are evaluated. Climatic and indoor temperatures are measured and compared against predicted ones using TRNSYS®, obtaining a 7% difference. A parametric study was conducted that varied floor temperatures to simulate radiant floor heating on the coolest day and nocturnal ventilation or/and radiant floor cooling on the hottest day in 2009. Results indicated that, during the winter, radiant floor heating increased the indoor air temperatures from 13.5ºC to 19.6ºC. During the summer, the indoor air temperature decreased from 32.1ºC to 27.4ºC at midnight, with a nocturnal ventilation of 5 ACH. Combining ventilation and radiant floor cooling decreased the indoor air temperatures to 26.9ºC (0.5ºC lower). As a result, the effect of nighttime ventilation was significant on indoor temperatures in the building; however, the effect of radiant floor cooling was almost negligible.

Key Words: *Office building, Radiant floor, Nocturnal ventilation, Conservation of energy.*

----------***----------

1. INTRODUCTION

Energy use in buildings accounts for 40% of total energy consumption. Developing countries are concerned over the augmented use of air conditioning systems [1]. Along with the increase in energy consumption, there are debates over whether air conditioned buildings should be recommended or prohibited due to discomfort (drafts, noise and impure air) [2].

In desert regions, energy consumption for thermal comfort conditions is very high. Some authors recommend using or managing passive or active techniques such as ventilation, radiant floor cooling or heating in order to decrease energy consumption and improve the indoor thermal environment in buildings during both summer and winter months [3]. Infiltration of air in buildings has been studied by McDowell et al. [4] to determine its impact on the thermal loads; they found that infiltration has a much higher negative impact on heating loads than on cooling loads. Also, management of passive cooling have a significant impact on the thermal summer comfort in a building [5]. Predictive control strategies improved the energy efficiency of intermittently heated radiant floor heating systems finding energy savings between 10% and 12% during cold winter months [6].

In 2006. Tian and Love [7] studied multi-floor radiant slab cooling through simulation and field measurements, reporting that even though radiant floor cooling has the potential to improve energy efficiency; it must be coordinated with air handling systems to avoid conflicts. However, radiant floor cooling systems are not recommended in humid climates because of condensation [8].

Very few authors have considered the combination of passive/active techniques such as nocturnal ventilation and radiant floor cooling. In 2000, Hayter and Torcellini [9] described a technique for designing and constructing low-energy buildings in which the HVAC design included radiant slab heating and natural ventilation cooling through an automatic window control, with a transpired solar collector (TSC) to preheat ventilation air for warehouses. However, Olesen et al. [10] found that the primary problem with combining radiant floor heating and displacement ventilation was inadvertently producing the opposite effects of the two systems; that is, if the floor temperature was too high, the supply air rose, reducing the ventilation effectiveness of the system and producing a mixing flow pattern in the room. If, however, the overheated floor is combined with displacement ventilation, the air could be supplied at a lower temperature for the ventilation system (depending on the external climate), with a resulting

reduction in the energy consumption [11]. Thus, the combination of active/passive techniques is not sufficiently studied.

The aim of this study is to study the effects of nocturnal ventilation and/or radiant floor cooling in summer and radiant floor heating in winter on the indoor air temperatures of a high thermal mass office building (heavyweight construction) located in an arid region.

2. CASE OF STUDY

The office building is a rectangular-shaped building of 1,114.96 m2, shown in Fig. 1, with its façade facing south. It is located in the city of Tabernas in Spain, at 37º 05' 27.8"N latitude and 2º 21' 19" W longitude. It lies at 555 m above sea level in a subtropical desert with scarce and irregular rain (200 mm per year), a high rate of irradiance (almost 3000 hours of sunlight per year) and large ambient temperature swings (12ºC). During 2009, the minimum monitored temperature was during January (-1.4ºC), and the maximum temperature was during July (41.7ºC).

Fig. 1. View of the office building and location of the monitored office.

2.1 Climate Conditions

A meteorological station installed on the roof of the building monitored the environmental climate conditions. Figures 2(a) and 2(b) show the average monthly solar radiation on the roof and south façade, the average monthly ambient temperature, the average monthly relative humidity and the average monthly wind velocity of 2009. Figure 2(a) shows that the monthly solar radiation was highest in June (7.66 kW-h/m^2) and July (7.63 kW-h/m^2); the average monthly solar radiation falling on the south façade was lower in summer and higher in winter as expected at this latitude. Average amount of sunshine was 14 hours during summer and 9 hours in winter. Figure 2(b) shows the average monthly ambient temperatures, humidity and wind velocities. Maximum average monthly temperature was in July (27.6ºC) and the minimum was in December (8.5ºC); lowest average monthly relative humidity was in June (40.1%) and highest was in October (71.2%). Average monthly wind velocity oscillated in the range of 2.3-3.1 m/s.

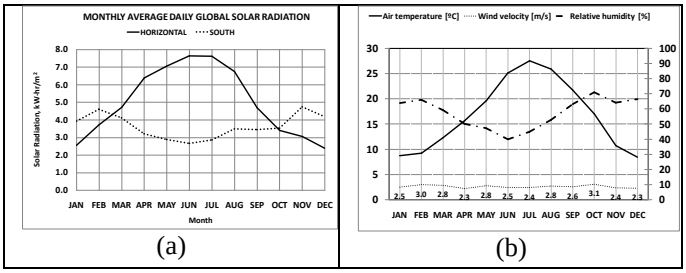

(a) (b)

Fig. 2. (a) Monthly global horizontal and southern solar radiation and (b) Monthly average wind velocity, ambient temperature and relative humidity for 2009.

2.2 Building Characteristics

The envelope of the building is constructed of thick multilayer composite walls to guarantee insulation, and the double-glazed aluminum framed windows are shaded to reduce the amplitude of the indoor temperature changes and prevent direct solar gains in summer. The south façade is protected by a 2 m projection (porch roof) to avoid direct beam radiation during the summer. More detailed features of the building were previously reported in [12].

Table 1 shows the construction materials of the walls and roof and their thermophysical properties. The composite wall is 44 cm thick, with an air gap at the center and polyurethane insulation material between the air gap and the hollow bricks. A Planitherm 4S® window (from Climalit Products), 4.63 m2 in size with a U-value of 3.21 W/m2K and a g-value of 0.722 is installed at the south wall. A 1 m wide overhang lies 1.5 m above the window to avoid direct sunshine on the window during summer.

Table 1. Building envelope components, dimensions and thermophysical properties

Material	L (m)	k (W/m K)	ρ (kg/m)^3	Cp, (kJ/kg K)
Walls				
Gypsum	0.02	1.08	900	1.00
Hollow brick	0.11	1.764	1200	0.90
Air	0.14			
Polyurethane	0.04	0.144	12	1.80
Hollow brick	0.11	1.764	1200	0.90
Mortar	0.02	5.04	2000	1.10
Roof				
Concrete	0.24	3.744	1500	1.00
Mortar	0.14	5.04	2000	1.10
Bitumen	0.005	0.828	1100	1.00
Polystyrene	0.04	0.144	25	1.50
Polypropylene	0.003	0.792	910	1.80
Gravel	0.06	2.916	1700	0.90
Floor				
Ceramic plate	0.25	3.78	1200	2.00
Mortar	0.04	5.04	2000	1.10
Sand	0.035	7.20	2000	1.00
Concrete	0.15	8.28	2300	1.00
Gravel	0.20	2.916	1700	0.90

The monitored office was chosen due to its location; it is located in the corner of the west end of the building as shown in Fig. 3(a). It is irradiated on the west and south walls, as well as the roof. The vertical and horizontal sketches of the cross section are shown in Figures 3(a) and 3(b). The north wall of the office is next to a long hall, and the east wall is adjacent to the subsequent office.

Fig. 3(a). West façade of the office

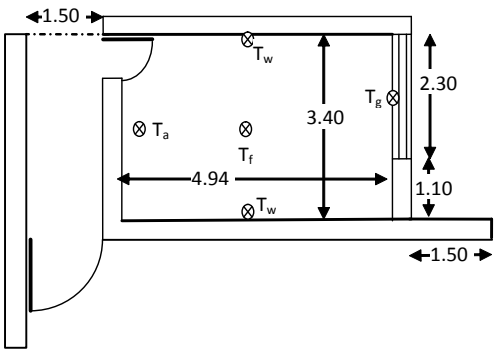

(b)

Fig. 3(b). Vertical cross-section of the office,

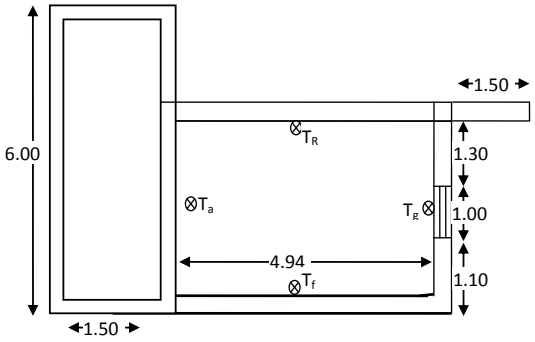

(c)

Fig. 3(c). West façade of the office.

3. THERMAL SIMULATION OF THE OFFICE

TRNSYS® program was used to simulate the thermal performance of the office. The following methodology was applied: 1) Two weekend days; one of extreme cold and another one of extreme hot temperatures of 2009 were chosen as the input data for TRNSYS®. 2) The building location, weather conditions, orientation, envelope components and dimensions were input into the TRNSYS® program, the indoor air temperatures of the office under a free-floating condition (no HVAC systems) were calculated and compared against those measured in order to calibrate the simulation. 3) A parametric study changing the ventilation rates and floor temperatures were carried out to predict the indoor air temperatures of the office. 4) Effects of every heating and cooling technique on the indoor air temperature were determined.

3.1 Days for the Simulation

Following the previous methodology, January 17th (the coolest day in winter) and Saturday, July 25th (the hottest day in summer) were the days for the simulation. Figures 5(a)-(d) show the horizontal and vertical solar radiation, ambient temperature, relative humidity and wind velocity, corresponding to January 17th and July 25th. It can be seen from Figures 5(b) and 5(d) that the ambient temperatures dropped during the night and increased during the day; temperature; swings, day and night, were close to 10°C on both days. In winter day, Figure 5(a) shows that the solar radiation on the horizontal surface is lower than the radiation on the south surfaces–as expected. Sunrise was at 8:00 hr; the solar radiation increased until 12:00 noon, then slowly decayed until 15:00 hr, when it abruptly dropped due to an obstruction on the roof relative to the position of the sun.

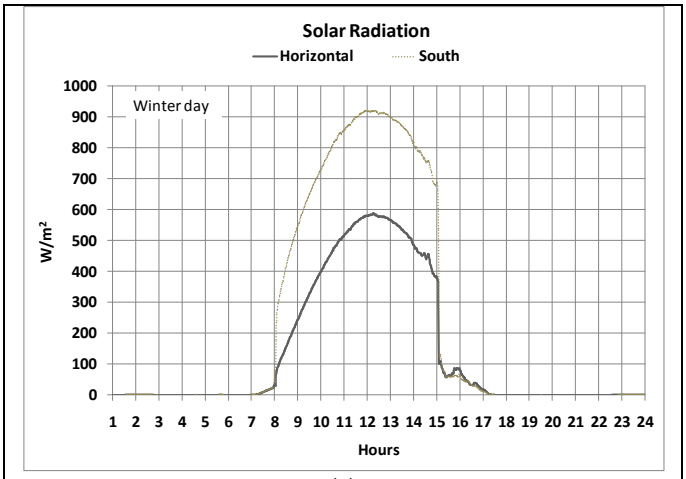

(a)

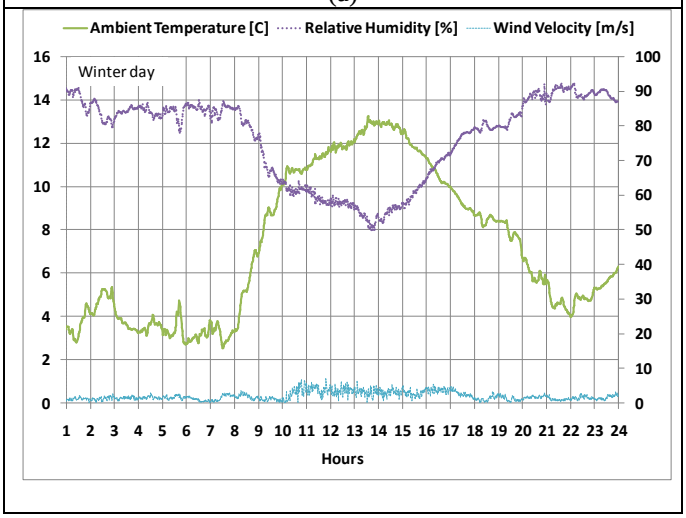

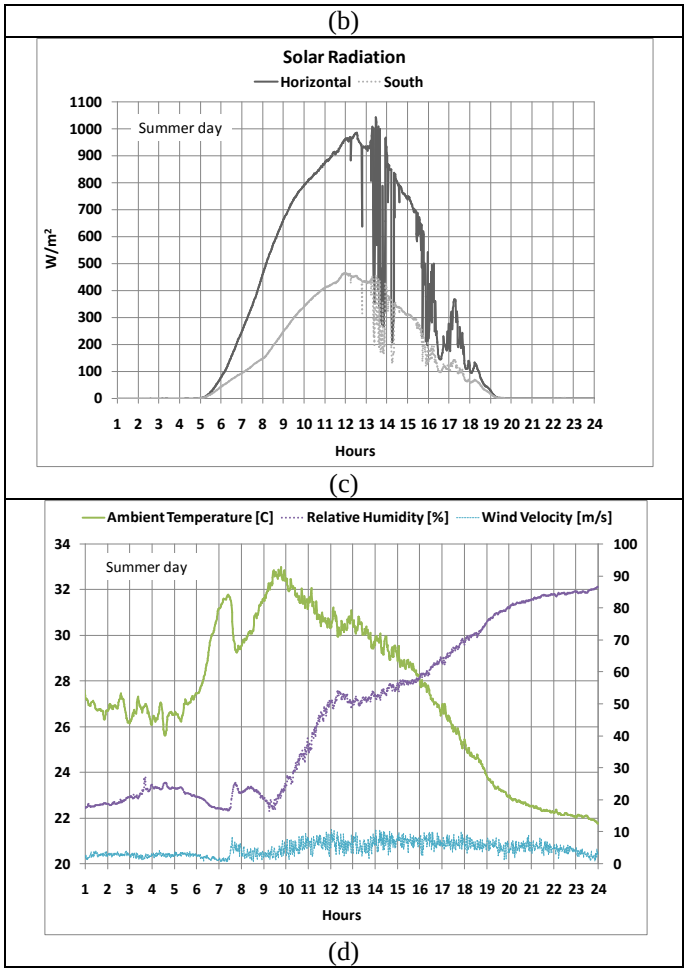

Fig. 5. (a) Incident solar radiation, (b) ambient temperature and relative humidity (January 17th); (c) solar radiation (d) ambient temperature and relative humidity (July 25th).

The ambient temperature was 2.5 ^{o}C after 7:00 hr during the night and early morning; increasing to 13.2^{o}C after 13:00 hr and then decreasing. The relative humidity was always higher at night (80-90%), decreasing during the day to 49% after 13:00 hr. Prior to 10:00 hr, as can be seen in Figure 5(b), the wind velocity was in the low range (<2.5 m/s) but then fluctuated, reaching a maximum of 6.9 m/s after 11:00 hr and decreasing (<3 m/s) after 17:00 hr.

In the summer day, Figure 5(c) shows the solar radiation on the horizontal and south surfaces. The solar radiation on the horizontal surface was higher than the radiation on the south surface; sunrise was at 5:00 hr, and the solar radiation steadily increased after 12:00 hr. It then abruptly fell during the afternoon, and the humidity increased, indicating cloudiness see Figure 5(d). The ambient temperature was low at night, ranging between 26-28 ^{o}C and then rising to 33 ^{o}C after 9:00hr; it then decreased after midnight to 21.8 ^{o}C, as expected due to cloudiness. The relative humidity was in the low range of 20-30 % at early morning and increased to 90 % at midnight; the wind velocity fluctuation was in the low range at night (<3.5 m/s) and early morning, increasing after 7:00 hr to a maximum of 10.8 m/s after 12:00 hr and remaining high until the oscillations decreased after 23:00 hr.

For the TRNSYS® simulation, the office was divided into two zones: Zone A (hallway) and Zone B (office), as shown in Figure 3(b). The east wall of Zone B was considered to be adiabatic (adjacent office), as well as the eastside of the Zone A; the measured solar radiation was input to Type 16 (Solar Radiation Processor). Envelope components of the office were input to Type 56 (Multi-Zone Building). TRNBuilt module was used to calculate the U-values for the wall. The U-values of the walls were 0.532 W/m² K for heat transfer coefficients of 7.7 W/m^2 K indoors and 25 W/m^2 K outdoors. The roof U-value was 0.621 W/m² K for 5.7 + 3.8V outdoors and 9.26 W/m² K indoors [15]. Absorptances of ceiling and walls were 0.3. Thermal capacitance of the office was 1000kJ/K (furniture + air), with lighting of 5 W/m2. An ACH ventilation of 0.25 was considered, as suggested by ANSI/ASHRAE-62 [16]. Simulations were performed every minute for 24 hrs and results were plotted every hour.

3.2 Measurement instruments of the office

Six temperature sensors were installed in the office; the sensor measuring the air temperature was located 1.5 m above the floor and 0.10 m away from the north wall; the other five were attached at the middle of the floor, on the glazing, on the east and west walls and in the middle of the roof, as shown in Figure 3(b) [13]. The measurement instruments and their descriptions are presented in Table 2.

Table 2. Instrumentation used for monitoring the office.

Sensor	Measured Variable	Description
2 Pyranometer, model CM11. Kipp and Zonen	Horizontal and vertical global Solar Irradiance	Spectral range from 285 to 2800 nm; Sensitivity of 7 to 14 µV/W/m².
1 Pygeometer, model CGR-4. Kipp and Zonen	Long wave radiation from the surface of the test component	Spectral range of 4500 to 42000 nm, 5 to 15 µV/W/m²; Response time of18 s; Temperature dependence of sensitivity (-20 ºC to +50 ºC) < 1%.
1 Sensor model WindSonic. Gill Instruments, LTD.	Wind velocity	Ultrasonic Output Rate of 0.25, 0.5, 1, 2, and 4 Hz; Wind Speed of 0-60 m/s;
1 Sensor model HMP45A/D. Vaisala.	Outdoor relative humidity	Range from 0.8 to 100%RH; Accuracy at +20 °C. Response time (90% at +20 °C) 10 s.
Platinum thermo-resistance, PT100	Air temperature	Accuracy: 1/10 DIN of Class B with a tolerance of ±0.3°C at 0°C.
Platinum thermo-	Surface temperature	Accuracy: 1/10 DIN of Class B with a tolerance

resistance, PT100		of ±0.3°C at 0°C.

A data acquisition system of 16-bit A/D resolution was used. The uncertainty, u(Ti), corresponding to the measurement of indoor air temperature, Ti, was calculated according to ISO 5725 [14]. The calculated air temperature uncertainty was 0.4°C with a 95% level of confidence, using a coverage factor of k*=2.

3.3 Comparison between measured and predicted indoor temperatures

Figures 6(a) and 6(b) show the mean ambient air temperature and the measured and predicted indoor air temperatures in both the winter and summer days, respectively.

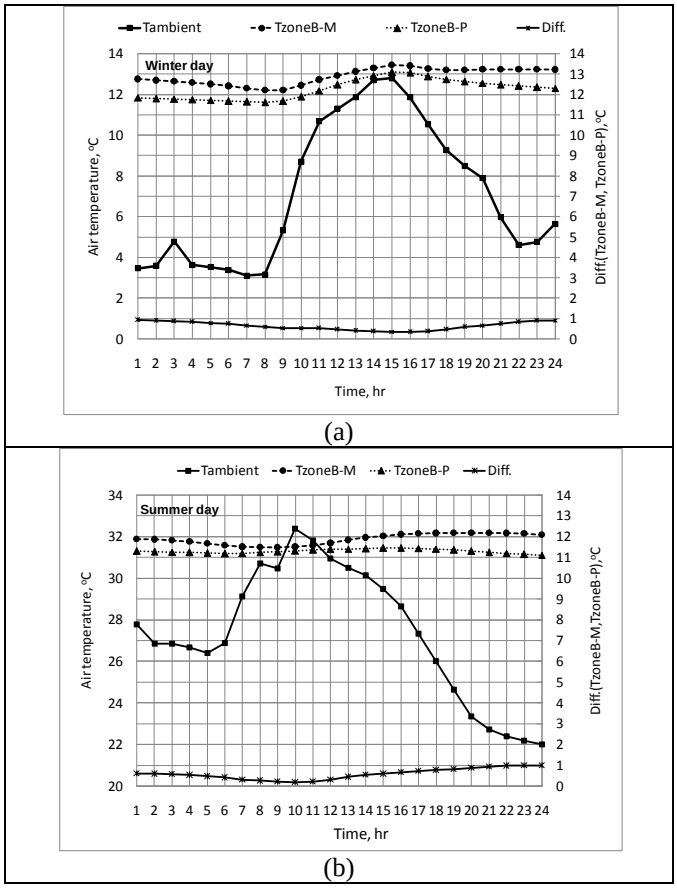

Fig 6. Ambient temperatures and monitored and predicted temperatures for (a) winter (Jan 17th) and (b) summer (July 25th).

Both Figures show that the predicted indoor air temperature of the office follows the same pattern of the measured one; the amplitude of the fluctuation compared to the ambient temperature was small due to the high thermal inertia of the envelope. As seen in Figure 6(a), the mean minimum outdoor ambient temperature was 3.1ºC at 7:00 hrs, and the maximum was 12.8ºC at 15:00 hrs a difference of 9.7ºC; the minimum and maximum mean measured temperatures were 12.2ºC at 8:00 hrs and 13.5ºC a difference of 1.3ºC; the minimum and maximum mean predicted temperatures were 11.6ºC at 8:00 hrs and 13.1ºC at 15:00 hrs a difference of 1.5ºC. A comparison between the measured and predicted indoor air temperatures indicates that their maximum difference was 0.9ºC (7.2%) at night and the minimum was 0.3ºC (2.5%), with a correlation coefficient of r^2=0.92. During the night, the indoor air temperatures were not as low as the outside ambient temperatures, demonstrating that the thermal inertia of the building plays an important role.

On the summer day, Figure 6(b) show that the maximum mean ambient temperature was 32.4ºC at 10:00 hrs, and the minimum was 22.0 ºC at 24:00hrs a difference of 10.4ºC. The maximum and minimum mean measured temperatures were 32.2ºC at 18:00 and 31.5ºC at 7:00 hrs—a difference of 0.7ºC; the maximum and minimum mean predicted temperatures were 31.5ºC at 15:00 hrs and 31.1ºC at 24:00—a difference of 0.4ºC. As previously noted, the indoor air temperature fluctuation is nearly negligible, so it is clear that heat accumulated inside the building. A comparison between the measured and predicted indoor air temperatures shows that their maximum difference was 1.0ºC (7.2%) at night, and their minimum difference was 0.2ºC (2.5%), with a correlation coefficient of r^2=0.92. The predicted and measured indoor air temperatures show very close agreement, thus calibrating the TRNSYS® program. These results show that it is necessary to remove the accumulated heat in the office during the summer. Therefore, nocturnal cooling is desirable for preventing overheating by taking advantage of the minimum outdoor air temperature.

4. PARAMETRIC STUDY

The parametric study considers three techniques: radiant floor heating and cooling and nocturnal ventilation. Radiant heating/cooling systems refer controlled surface floor temperature. To simulate the radiant floor heating or cooling, the *measured floor temperature* were taken as *floor base temperature* and increased for heating or decreased for cooling in the simulation. Nocturnal ventilation refers to cooler air driven into the building during the night, reducing temperatures in the building. Normally, ventilation rates are measured by AHC (Air Changes per Hour) [16].

4.1. Effect radiant floor heating

For the winter day, two cases were considered: 1) the measured floor temperature, $T_{floor\text{-}M}$, were increased by 5ºC, 10ºC and 15ºC during 9:00 to 18:00 hrs, and 2) the same but for 24 hrs. Figures 7(a) and 7(b) show the ambient temperatures (T_{amb}), *floor base temperature* ($T_{floor\text{-}M}$), indoor measured air temperatures ($T_{zoneB\text{-}M}$) and the predicted one (T_{zoneB}) for cases 1) and 2), respectively. As can be seen in Figure 7(a), increasing $T_{floor\ -M}$, by 5ºC, 10ºC and 15ºC during 9 hours resulted in increments of indoor air temperatures (T_{zoneB}) of 0.3ºC, 1.2ºC and 2.2ºC on average, respectively.

Figure 7(a) shows that an increment of 15ºC of the *floor base temperature* increased the indoor air temperature to a maximum of 15.8^{o}C at 15:00 hr, against the outdoor ambient temperature of 12.8^{o}C. Similar results are presented by Figure 7(b), but for 24 hours of floor heating. The augmentation of the *floor base temperatures* of the office by increments of 5^{o}C, 10^{o}C and 15^{o}C caused the increase in the indoor air temperatures in increments of 1.5^{o}C, 3.7^{o}C and 5.8^{o}C on average, respectively. For increments of 15ºC for 24 hours, the minimum indoor air temperature reached was 18.1^{o}C and the maximum was 19.6^{o}C at 15:00 hrs. The indoor air temperatures were in the low range (18^{o}C-20^{o}C) of acceptable temperatures [17].

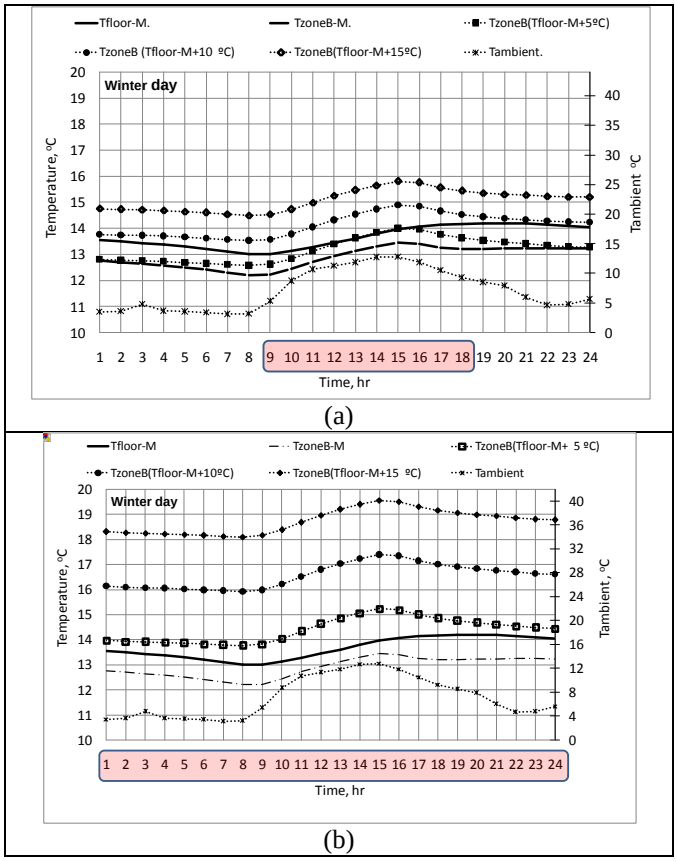

Fig. 7. Ambient temperature, measured floor and indoor temperatures and predicted indoor temperatures for different radiant heating floor temperatures from (a) 9-18 hrs and (b) 0-24 hrs.

4.2. Effect of radiant floor cooling

For the summer day, three cases were considered for the simulation: 1) *floor base temperature* of the office decreased by 1^{o}C, 2^{o}C, 3^{o}C, 4^{o}C and 5^{o}C, during 9:00 to 18:00 hrs, 2) nocturnal ventilation rates of 1, 2, 3, 4 and 5 ACH from 20:00 to 6:00 hrs and 3) a combination of these two techniques. Figures 8(a) and 8(b) show the ambient temperature, the *floor base temperature* and indoor temperature against the predicted one for cases 1) and 2). Both figures show that the oscillation of the indoor measured air temperature of the office (31.5^{o}C-32.2^{o}C) was lower than the oscillation of the ambient temperatures (22.0 ^{o}C-32.4 ^{o}C). The indoor air temperatures were always higher than outdoor air temperatures, indicating that heat was accumulating inside the office and therefore throughout the building.

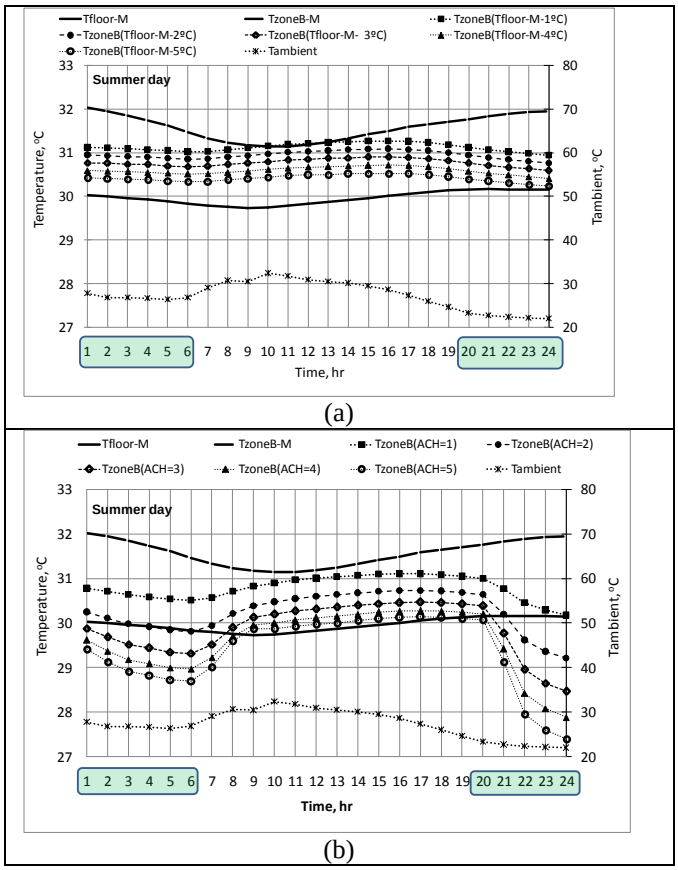

Fig. 8. (a) Ambient temperature, *floor base temperature* and indoor measured air temperatures and predicted ones for different radiant cooling floor temperatures from 20-6 hrs and (b) for different infiltration rates from 20-6 hrs.

For case 1), Figure 8(a), shows that *floor base temperature* decrements of 1^{o}C, 2^{o}C, 3^{o}C, 4^{o}C and 5^{o}C from 9:00-18:00 hrs causes decrements of the indoor air temperatures of 0.7^{o}C, 0.9^{o}C, 1.1^{o}C, 1.3^{o}C and 1.5^{o}C respectively. In this case, the predicted minimum indoor air temperature was 30.2^{o}C at midnight, which represented a very small decrease in 1.9^{o}C. For case 2, Figure 8(b), shows the effect of nocturnal ventilation rates on indoor air temperatures. As seen in this figure, the predicted indoor air temperatures at the office rapidly decreased at night. For nocturnal ACH ventilation rates of 1, 2, 3, 4 and 5 (from 20:00 to 6:00 hrs), the decrement of the indoor air temperatures was 1.1^{o}C, 1.6^{o}C, 2.0^{o}C, 2.3^{o}C, 2.5^{o}C respectively. During the night, for an ACH rate of 5, the lowest predicted indoor air temperature was 27.4^{o}C, which represented a decrease of 4.7^{o}C; during daylight. Thus, nocturnal ventilation techniques are very important in hot arid climates during the summer.

4.3. Effects of night ventilation and radiant floor cooling

Figure 9 presents the ambient temperatures, the base floor and indoor air temperatures against the predicted ones for case 3). The notation is as follows: $T_{zoneB\ (1,\ -1)}$ indicates temperatures at an ACH value of 1, the -1 indicates the *floor base temperature* minus 1°C; the same notation is used for the other four cases. The simulation results in Figure 9 showed that for cases (1,-1), (2,-2), (3,-3), (4,-4) and (5,-5), the decrements of the *floor base temperatures* were 1.2°C, 1.9°C, 2.4°C, 2.8°C and 3.1°C respectively. It is noted that for case (5,-5), the office air temperature decreased from 32.1°C to 26.9°C, indicating a maximum temperature drop of 5.2°C.

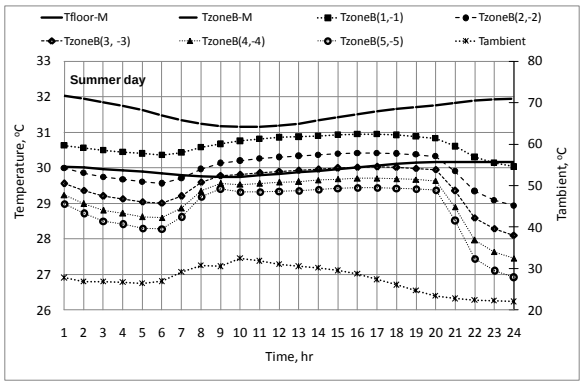

Fig. 9. Ambient temperature, monitored floor and room air temperatures and simulated room air temperatures for the combination of infiltration and radiant cooling floor from 20:00-6:00 hrs.

Comparing this result against the ones of Figure 8(b) (considering only ventilation), it shows a slight decrease of indoor air temperature of only 0.5°C. Therefore, the effect of radiant floor cooling on the indoor air temperature was negligible compared to nocturnal ventilation.

4. CONCLUSIONS

The effects of the combination of night ventilation and radiant floor cooling/heating on indoor air temperatures of a high thermal mass office building located in a hot arid region were evaluated. Simulated results indicated that the predicted indoor temperatures against measured ones showed closed agreement, between 7.2% for winter and 3.1% for summer.

In the winter day, considering radiant floor heating showed a maximum increment of 5.8°C in the indoor air temperature (maximum indoor air temperature reached was 19.6°C).

In the summer day, considering radiant floor cooling showed a maximum increment of 1.5°C on average, indicating that radiant floor cooling had no significant effect on diminishing the indoor air temperatures. Considering nocturnal ventilation for an ACH rate of 5, the air temperature of the office decreased at midnight to 27.4°C, a maximum temperature drop of 4.7°C. Combining both techniques, the lowest indoor air temperature was 26.9°C during the night, a temperature drop of 5.2°C.

Thus, nocturnal ventilation is imperative in hot arid regions to reduce (or even avoid) the use of HVAC systems. On the other hand, radiant floor heating is highly recommended in the winter.

ACKNOWLEDGEMENT

The authors are grateful to the AECID (*Agencia Española para la Cooperación Internacional y el Desarrollo*) for the financial support provided to projects PCI-A/019437/08 and PCI-A/025/63/09.

REFERENCES

[1] IEA, 2006. International En ergy Agency (IEA). Key World Energy Statistics.

[2] Nezhad, H.G. 2009. World Energy Scenarios for the year 2010. Journal of Strategic Planning for Energy and Environment, 9 (4), 26-44.

[3] Al-Rabghia, O. M. and Hittle, D. C., 2001. Energy simulation in buildings: overview and BLAST example. *Energy Conversion and Management.*42, 1623–1635.

[4] McDowell, T., Thornton, J., Emmerich, S. and Walton, G., 2003. Integration of Airflow and Energy Simulation using CONTAM and TRNSYS. National Institute of Standards and Technology, Gaithersburg, MD. Thermal Energy System Specialists, Madison, Wisc.*ASHRAE Transactions* 109, KC-03-10-2.

[5] Breesch, H., Bossaer, A and Janssens, A., 2005. Passive cooling in a low-energy office building.*Solar Energy* 79, 682-696.

[6] Cho, S. H. and Zaheer-uddin, M., 2003. Predictive control of intermittently operated radiant floor heating systems. *Energy Conversion and Management*. 44, 1333–1342.

[7] Tian, Z. and Love, , J.A., Aug. 2006. *Radiant slab cooling: a case study of building energy performance*. 2nd. National IBPSA-USA Conference, Cambridge, MA, USA, 2-4.

[8] Song, D., Kimb, T., Song, S., Hwang, S. and Leighd, S. B., 2008. Performance evaluation of a radiant floor cooling system integrated with dehumidified ventilation. *Applied Thermal Engineering* 28, 1299-1311.

[9] Hayter, S. J. and Torcellini, P.A., Aug 2000. A Case Study of the Energy Design Process Used for A Retail Application. NREL/CP-550-28129. *Conference American Solar Energy Society. (ASES)* Madison, Wisconsin.

[10] Olesen, B. W., Sommer, K., Düchting B., 2002. *Control of Slab Heating and Cooling Systems Studied by Dynamic Computer Simulations.ASHRAE Transactions*, 108, Pt. 2.

[11] Causone, F., Baldin, F., Olesen, B. W. and Corgnati, S.P., 2010. Floor heating and cooling combined with displacement ventilation: Possibilities and limitations. *Energy and Buildings* 42, 2338–2352.

[12] Palero, S., San Juan, C., Enríquez, R.Ferrer, J. A, Soutullo, S., Martí, J., Bosqued, A., Guzmán, J. D., Jiménez, M.J, Bosqued, R., Porcar, B. and Heras, M.R., 2006.*Thorough Study of a Proposal to Improve the Thermal Behaviour of a Bioclimatic Building*. Presented at 23rd. International Conference on Passive and Low Energy Architecture. Switzerland. 6-8 September.

[13] Jiménez, M.J., Enríquez, R., Olmedo, N., Sánchez, N. andHeras, M.R., 2010. *Monitorizacionenergetica de los C-DdIs del PSE-ARFRISOL*.Diseño experimental. In Spanish. Presented at congress "*1st. Congress on Bioclimatic Architecture and Solar Cooling*. 23-26.

[14] ISO Standard 5725, 1995. *ISO Guide to the expression of uncertainty in measurement*. Ginebra. ISBN 92-67-10188-9.

[15] TRNSYS 16 Manual, 2006.Solar Energy Laboratory, Univ. of Wisconsin-Madison. http://sel.me.wisc.edu/trnsys

[16] ANSI/ASHRAE, standard 62, 2001.*Ventilation for Acceptable Indoor Air Quality.*

[17] ASHRAE 55, 2004. *Thermal and environmental conditions for human occupancy.*

BIOGRAPHIES

Gabriela del S. Álvarez García. Dr. in Engineering. Professor at ME Dept., Cenidet-ITM. Mexico. She has several publications in reputed international journals. Research and teaching of heat transfer, conjugate heat and mass transfer, experimental methods applied to passive/active systems for conservation of energy.

Maria José Jimenez Taboada. Dr. in Physical Sciences. Researcher in Ciemat, Spain. She has several publications in reputed international journals. She does research in energy efficiency in buildings, integration of solar systems in buildings, experimental methods and analysis, thermal monitoring of buildings.

María del Rosario Heras Celemín. Dr. in Physical Sciences. She is a researcher in Ciemat, Spain. She has several publications in reputed international journals. Research in Applied Physics, energy efficiency in buildings. Solar energy applied to buildings.

Miguel Angel Chagolla Gaona. Dr. in Mechanical Engineering. Professor of Zacatepec Tecnology Institute-TNM. Research in solar energy in buildings, measurement of climatic conditions and building simulation.

Jesus Arce Landa. Dr. in Engineering. Professor at ME Dept., CENIDET Mexico. He has publications in reputed international journals. Research in thermal and thermodynamical systems, solar energy, conservation of energy, passive ventilation using solar chimneys.

Jesus P. Xaman Villaseñor. Dr. in Mechanical Engineering. Professor at ME Dept., CENIDET Mexico. He has publications in reputed international journals. Research in conjugate heat transfer problems, CFD, turbulence, passive and active systems, ventilation.